THE JOURNAL OF PHYSICAL CHEMISTRY B

Article

pubs.acs.org/JPCB

Hydration Dynamics of Aqueous Nitrate

Jan Thøgersen,*[,†] Julien Réhault,[‡] Michael Odelius,*[,§] Tom Ogden,[§] Naresh K. Jena,[§] Svend J. Knak Jensen,[†] Søren R. Keiding,[†] and Jan Helbing*[,‡]

[†]Department of Chemistry, Aarhus University, Langelandsgade 140, DK-8000 Aarhus, Denmark

[‡]Institute of Physical Chemistry, University of Zürich, Winterthurerstrasse 190, CH-8057, Zürich, Switzerland

[§]Department of Physics, Albanova, Roslagstullbacken 21, Stockholm University, SE-106 91 Stockholm, Sweden

ABSTRACT: Aqueous nitrate, NO_3^-(aq), was studied by 2D-IR, UV−IR, and UV−UV time-resolved spectroscopies in combination with molecular dynamics (MD) simulations with the purpose of determining the hydration dynamics around the anion. In water, the D_{3h} symmetry of NO_3^- is broken, and the degeneracy of the asymmetric-stretch modes is lifted. This provides a very sensitive probe of the ion−water interactions. The 2D-IR measurements reveal excitation exchange between the two nondegenerate asymmetric-stretch vibrations on a 300-fs time scale concomitant with fast anisotropy decay of the diagonal-peak signals. The MD simulations show that this is caused by jumps of the transition dipole orientations related to fluctuations of the hydrogen bonds connecting the nitrate ion to the nearest water molecules. Reorientation of the ion, which is associated with the hydrogen-bond breaking, was monitored by time-resolved UV−IR and UV−UV spectroscopy, revealing a 2-ps time constant. These time scales are very similar to those reported for isotope-labeled water, suggesting that NO_3^-(aq) has a labile hydration shell.

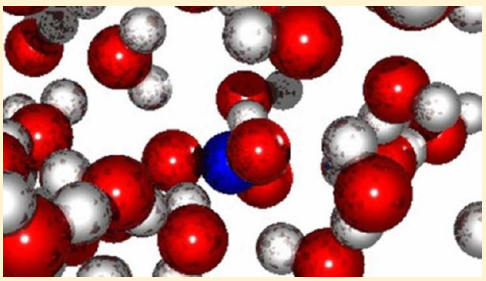

INTRODUCTION

When ions are dissolved in water, they can interact strongly with the nearest water molecules and influence the hydrogen-bond network between the water molecules. This process is called hydration, and the water molecules are said to form hydration shells around the ions. Hydrated ions are omnipresent on Earth. From hydration of salts in the oceans to ion transport through cellular membranes, the success of a vast number of chemical and biological processes relies decisively on the mechanisms of hydration. Decades of intensive research have greatly advanced the understanding of how ions are hydrated,[1−3] yet fundamental questions remain unanswered. Central to the ongoing studies is the extent to which the hydration shells are stable with long lasting ion−water hydrogen bonds, or labile with frequent exchanges of molecules, and how these processes determine the angular and translational mobility of the ions.

In neat liquid water, the molecules are interconnected by a network of hydrogen bonds linking a hydrogen atom of one molecule to an oxygen atom of another. The hydrogen bonds are 10−100 times weaker than the covalent bonds within a water molecule, and each water molecule can form hydrogen bonds with up to four neighboring water molecules. At room temperature, the hydrogen-bond lengths and angles fluctuate strongly on a subpicosecond time scale,[4,5] but these fluctuations result in only modest changes in the local water structure. However, sometimes, a hydrogen bond is broken, and a bond to a new partner is formed concomitant with the reorientation of the water molecule.[6] The water molecules reorient on average every 2.5 ps,[7] and the hydrogen bonds thus fluctuate several times before reorientation occurs. Recent models developed from molecular dynamics simulations[8] indicate that the reorientation mainly occurs in sudden large-angle jumps involving the concerted cleaving and formation of hydrogen bonds. Direct verification of this picture is difficult to obtain from experiments in neat water,[9] but the models are able to reconcile seemingly contradictory reorientation time constants derived from nuclear magnetic resonance (NMR), infrared (IR), and neutron-scattering data.[10] On the other hand, experimental evidence that a jump mechanism is responsible for the reorientation of water in the solvation shell of ions has recently been presented.[11,12]

The hydrogen-bond network changes considerably when ions are dissolved in water. Although the question of whether the bulk water network is affected is still debated,[12−18] several studies of hydrated ions indicate that the nearby water molecules form quasistable hydration shells with ion−water hydrogen bonds lasting much longer than the hydrogen bonds of neat water.[18,19] In the case of Br^-(aq),[20] the hydrogen shell was found to remain intact for 5 ps, while the hydration shells of BF_4^-(aq)[19] and ClO_4^- (aq)[18] exchange water molecules, on average, every 7 ps. Polarization-sensitive two-dimensional infrared (2D-IR) spectroscopy in combination with Car−Parrinello molecular dynamics modeling suggests that the water molecules that are hydrogen-bonded to the ion reorient in sudden large-angle jumps involving the concerted breaking of a hydrogen bond to the ion and formation of a hydrogen bond to a water molecule in the second hydration shell.[11] Between the

Received: October 12, 2012
Revised: March 4, 2013
Published: March 5, 2013

   dx.doi.org/10.1021/jp310090u | J. Phys. Chem. B 2013, 117, 3376−3388

angular jumps, the water molecules slowly reorient with the ion in an intact ion−water shell.

The present study concerns the hydration dynamics of aqueous nitrate, NO_3^-(aq). In contrast to ions such as BF_4^-(aq)[19] and ClO_4^-(aq),[18] there is no distinct fingerprint for hydrogen bonding to NO_3^-(aq) in the OH stretch spectrum of water, which is therefore not a suitable probe. Nevertheless, aqueous nitrate is an excellent molecule for studying ionic hydration shell dynamics, because its spectroscopic properties depend strongly on the hydrogen-bonding interactions with the surrounding water, which lift the degeneracy of the two asymmetric-stretch vibrations.[21] Hence, contrary to most previous experiments, which have measured the dynamics of the ion−water hydrogen bonds by vibrational spectroscopy of the water molecules, the present experiments probe the spectral signatures of the ion. This yields information on the hydrogen bonds connected to the molecular anion with little, if any, background signal from the bulk solvent.

Previously, line-shape analysis of polarized Raman spectra and their temperature dependence has been used to derive picosecond reorientation time constants for several molecular ions in water including nitrate.[22] Here, we use 2D-IR and pump−probe spectroscopy to investigate the fluctuations in the ion−water hydrogen bonds, the intramolecular coupling of the vibrational modes of nitrate, and the reorientation of the nitrate molecules. A similar approach was recently taken by Vorobyev et al., who investigated the water-induced relaxation of guanidinium (D_3 symmetry).[23] Use of the nitrate ion offers the advantage of a much larger solvent-induced splitting of the degenerate vibrations, already present in pure water, which also allows excitation-transfer and normal-mode-mixing processes to be better differentiated.

The quality of our 2D-IR data deteriorates for time scales longer than 1 ps, because of a background signal from scattered light and the short lifetime of the vibrational states. Reorientation dynamics occurring on longer time scales were therefore monitored by time-resolved spectroscopy involving excitation of the electronically excited states of nitrate. Thus, UV pump−UV probe and UV pump−IR probe transient absorption spectroscopies can follow the nitrate−water interactions for up to 10 ps. The experimental findings were interpreted with the aid of both classical molecular dynamics (MD) simulations and Car−Parrinello molecular dynamics (CPMD) simulations. The combination of time-resolved 2D-IR, UV−UV, and UV−IR spectroscopies with molecular dynamics simulations provides a comprehensive and consistent description of the hydration of aqueous nitrate.

EXPERIMENTAL SECTION

Measurements involving UV excitation were carried out at the University of Aarhus (Aarhus, Denmark), whereas 2D-IR experiments were performed at the University of Zürich (Zürich, Switzerland). Each laboratory utilized a 1-kHz amplified Ti:sapphire laser system emitting 100-fs pulses at 800 nm with an energy of about 1 mJ.

The two-dimensional infrared (2D-IR) spectrometer in Zürich used a beam of midinfrared femtosecond pulses from an optical parametric amplifier (OPA). Two reflections off a wedged BaF_2 window produced the probe and reference beams. Pairs of collinear pump pulses were generated by a fast-scanning interferometer with automated phase determination.[24] These pulses passed a computer-controlled waveplate, which was rotated at regular intervals (approximately 20 s), switching the pump polarization between parallel and perpendicular orientations relative to the polarization of the probe pulses for the quasisimultaneous recording of spectra of different polarization conditions. Probe and reference beams were then spectrally dispersed in a monochromator and detected by a double-array detector on a single-shot basis as a function of the coherence time, t_1, between the pump pulses and the waiting time, t_2, between the second pump pulse and the probe pulse. Fourier transformation along t_1 directly yielded absorptive 2D-IR spectra.

Two types of transient absorption measurements were performed in Aarhus: UV pump−UV probe and UV pump−IR probe. Both measurements utilized 200-nm pump pulses of 200-fs duration generated by frequency quadrupling the 800-nm laser pulses in three consecutive frequency-doubling and sum-frequency-mixing β-BaB_2O_4 (BBO) crystals. The pump pulses were sent through a scanning delay line and a $\lambda/2$ waveplate before they were focused through the sample by a concave mirror. The beam of 195-nm UV probe pulses was generated by frequency upconverting the output of an OPA and then split into a signal beam and a reference beam. The signal beam was focused on the sample by a concave mirror, thus probing the sample inside the area defined by the pump beam, whereas the reference beam bypassed the sample. Signal and reference pulses were subsequently detected by matched photodiodes. The anisotropy data were derived from individual transient absorption measurements recorded with parallel ($\Delta A_\parallel$) and perpendicular ($\Delta A_\perp$) pump and probe polarizations.

For UV pump−IR probe spectroscopy, IR probe pulses covering the entire asymmetric-stretch absorption band of NO_3^- (see Figure 1) were generated by difference frequency mixing the output pulses from an OPA. The probe beam was divided into signal and reference beams by a silicon beam splitter. The signal beam probed the sample inside the volume excited by the UV pump pulse, whereas the reference beam passed through the sample above the pump beam. The polarization of the ultraviolet pump beam was fixed at 45° with respect to that of the infrared probe pulse. An analyzing polarizer interchangeably selected the infrared signal and reference components parallel and perpendicular to the polarization of the pump beam, allowing the absorption changes induced parallel ($\Delta A_\parallel$) and perpendicular ($\Delta A_\perp$) to the pump-pulse polarization to be measured by a spectrometer

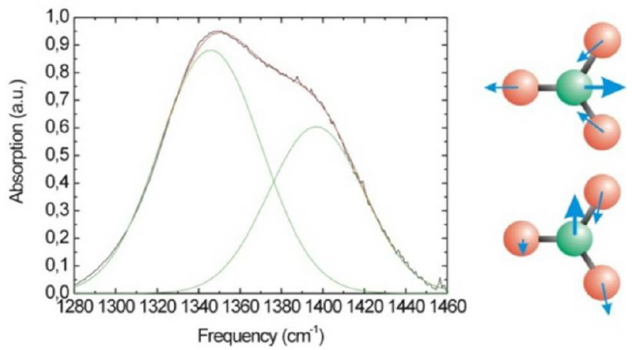

Figure 1. Infrared absorption spectrum of NO_3^-(aq) (black line). Green and red lines represent a fit with two Gaussian functions. The arrows in the molecular pictures to the right indicate the atomic displacement vectors for the degenerate asymmetric-stretch vibrations.

dx.doi.org/10.1021/jp310090u | J. Phys. Chem. B 2013, 117, 3376−3388

equipped with a double-array detector. Each measurement consisted of many consecutive pump−probe delay scans. The analyzing polarizer was rotated between each scan for quasisimultaneous recording of $\Delta A_{\parallel}$ and $\Delta A_{\perp}$.

The samples used in Aarhus consisted of a constantly flowing film of 14 mM (UV pump−UV probe) or 0.1 M (UV pump−IR probe) aqueous KNO_3 solution suspended between two parallel, 50-μm-thick titanium wires separated by 4 mm.[25] For the 2D-IR experiments, a 1 M aqueous solution of $NaNO_3$ was sandwiched between two 2-mm-thick CaF_2 windows with a 6-μm spacer. The peak absorption of the asymmetric-stretch band of NO_3^- was approximately 0.3 on a broad water background of roughly the same size. Control experiments were carried out without the spacer, yielding samples of approximately 0.5-μm thickness, and in D_2O. No significant differences were observed. Furthermore, the band shapes of the background-corrected asymmetric-stretch bands of NO_3^-(aq) in the FTIR spectrum at concentrations of 0.1 and 1 M were identical.

THEORETICAL SECTION

Molecular dynamics simulations were performed to elucidate the connection between hydrogen-bond fluctuations and spectral dynamics, the splitting of the asymmetric N−O stretch band, and the reorientation of the NO_3^-(aq) transition moments. First, to investigate the concentration dependence and finite-size effects, classical MD simulations at 298 K were performed for several nanoseconds on an electrolyte solution of K^+ and NO_3^- in 55 and 550 water molecules, corresponding to 0.1 and 1.0 M concentrations, respectively, at densities of 1.0 and 1.05522 g/cm^3.[26] The force-field parameters for water and the potassium cation were provided by the M.Dyna*Mix* database,[27] and the force field for the nitrate ion was built from intermolecular and intramolecular potentials from refs 28 and 29. The size dependence was studied by comparing the solute−solvent radial distribution functions, which showed small differences between the small and large classical MD simulations. Having confirmed that the small system was large enough to describe the solvation structure, Car−Parrinello MD (CPMD) simulations were initialized from the small classical MD simulation.[30,31] The results from both classical MD and CPMD simulations were used in the analysis of the experimental data.

In the CPMD simulations, all water molecules were deuterated to ensure a small spectral overlap between the electronic and nuclear degrees of freedom. A time step of 1 fs was used in combination with a fictitious energy mass of 500 au and a Nosé−Hoover thermostat (2500 cm^{-1}) coupling to the OD vibrations. After a 20-ps equilibration run initialized from the classical MD results, the production run was conducted for 18.9 ps at 300 K. An analogous CPMD simulation at 350 K was equilibrated for 20 ps, after a period of elevated temperature. We used the BLYP functional, norm-conserving Troullier−Martins pseudopotentials (using a semicore description with maximum angular momentum and local p component for potassium) and a plane-wave expansion of the Kohn−Sham orbitals with truncation at an energy cutoff of 70 Ry.

Quantum chemical calculations on small clusters cut out in a 5-Å radius around the NO_3^- ion were used to sample vibrational spectra along the classical MD and the CPMD simulation trajectories. In Gaussian 09,[32] partial optimization and vibrational analysis at the BLYP/aug-cc-pVDZ level of approximation were performed on NO_3^- in a solvent environment at a frozen geometry for 180 configurations along each trajectory. (The basis set convergence of the results was confirmed by calculations with aug-cc-pVTZ, which reproduced the relative changes in the vibrations for the different configurations within a few wavenumbers.) For the vibrational modes, frequencies and dipole derivatives were used to simulate the IR spectrum and to study the orientational fluctuations in the molecular frame. The fluctuations in the vibrational modes were similar in the classical MD and CPMD simulations, so we display only the CPMD results. An ad hoc constant shift was applied to calculated IR frequencies in the comparison to experiment.

SPECTROSCOPY

Before presenting the experimental results, we provide a brief overview of the spectroscopy of the nitrate ion. The isolated nitrate ion is planar (D_{3h}) with the excess negative charge delocalized over the molecule, and accordingly, the two asymmetric-stretch vibrations are degenerate. Hydration breaks the molecular symmetry and lifts the degeneracy,[21,33] giving rise to the two absorption bands near 1350 and 1400 cm^{-1} shown in Figure 1.

Conceptually, the mechanism for the splitting of the asymmetrical stretch vibrations can be formulated in terms of the individual N−O groups. Through intermolecular interactions, primarily hydrogen bonding of the oxygen atoms in NO_3^- but also long-range electrostatic fields, the N−O groups experience variations in the shape of the stretching potentials. The three N−O stretches couple to give rise to a symmetric-stretch and two asymmetric-stretch normal modes, with small contributions from in-plane bending vibrations. These normal modes are sensitive to the differences in the N−O potentials. Thus, the symmetric-stretch mode (near 1100 cm^{-1}) is no longer fully symmetric, and the asymmetric-stretch modes become nondegenerate. They can still be pictured, however, as orthogonal linear combinations of the degenerate gas-phase modes sketched in Figure 1, and their transition dipole moments lie in the molecular plane and are perpendicular to each other.

To illustrate the sensitivity of the asymmetric N−O stretch band of NO_3^- to hydrogen-bonding interactions, we used electron structure calculations at the MP2/6-311+G(d,p) level to study the frequency splitting of the asymmetric-stretch absorption band pertaining to the complexes of NO_3^- and a single uncomplicated molecule/atom, X, from the first two periods of the periodic table. The calculated splitting was then related to ΔG°. The trend of the data in Figure 2 shows that the frequency splitting increases steadily from nearly 0 cm^{-1} for molecules without a permanent dipole moment, such as N_2, to 150 cm^{-1} for strongly hydrogen-bonding species such as HF.

Previously, the splitting of the asymmetric-stretch vibrations of NO_3^- was calculated for clusters of nitrate with one or two water molecules,[34] which underestimated the experimental value for the bulk solvent. It was speculated that, in aqueous solution, transient charge localization might lead to strong, highly asymmetric H-bonding involving mainly one N−O group. Indeed, recent ab initio MD simulations studying the structure and dynamics in the hydration shell of NO_3^- show that there is, instantaneously, a substantial asymmetry in the hydration both in structure and in dynamics.[35] The asymmetry in hydrogen bonding is correlated with transient elongations of individual N−O bonds associated with a charge redistribution in the NO_3^- ion.[36] Size-selective infrared multiple-photon photodissociation spectra of $NO_3^-(H_2O)_n$ clusters provide a

dx.doi.org/10.1021/jp310090u | J. Phys. Chem. B 2013, 117, 3376−3388

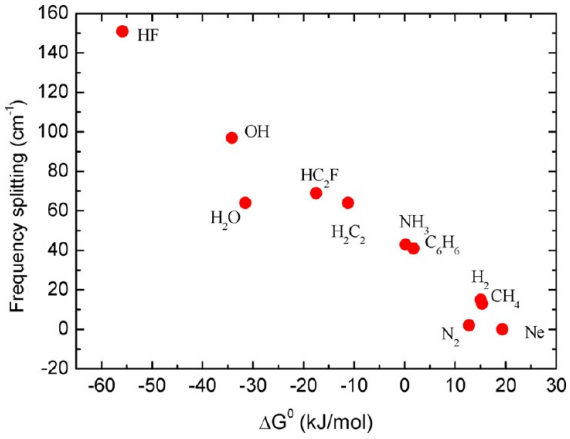

Figure 2. Calculated frequency splitting of the asymmetric-stretch vibrations of nitrate, induced by binding to the solvent molecule. The calculations were performed using Gaussian 09 at the MP2/G-311+G(d,p) level on the reaction $NO_3^- + X \rightarrow [\ NO_3X]^-$.

beautiful experimental demonstration of the effect of symmetry in the hydration of the nitrate ion.[37] They show a strong splitting of the asymmetric-stretch mode for n = 1, 2, and 5, but only a single resonance for n = 3, when all three oxygen atoms appear to form similar hydrogen bonds. These results suggest that transient fluctuations of the strength or geometry of the hydrogen bonds between the nitrate anions and the water molecules in the hydration shell will be reflected very sensitively in the linear and nonlinear infrared spectra of the asymmetric-stretch vibrations.

RESULTS

2D-IR Spectroscopy. The 2D-IR data were recorded by exciting and probing the fundamental asymmetric-stretch transitions of aqueous nitrate with infrared laser pulses covering the entire absorption band. The measurements were taken with parallel and perpendicular polarizations of the pump and probe pulses. Figure 3 shows the 2D-IR spectra of NO_3^-(aq) for a number of time delays between excitation and probing of the asymmetric-stretch vibrations. Data recorded with parallel ($\Delta A_{\parallel}$) and perpendicular ($\Delta A_{\perp}$) polarization of pump and probe beams are shown in the first two columns. The magic-angle signals, ΔA_{MA}, were calculated from these data using $\Delta A_{MA} = \Delta A_{\parallel} + 2\Delta A_{\perp}$ and are plotted in the third column. They show intensity changes free of reorientation effects. All spectra were normalized to the minimum negative signal for better comparison. The negative components of the diagonal signals at excitation wavenumbers of 1340 and 1400 cm^{-1} reflect the asymmetric-stretch absorption maxima of the spectrum in Figure 1. These signals are due to the pump-induced bleaching of ground-state nitrate ions and stimulated emission from the first excited states of the asymmetric-stretch vibrations. Because of band overlap, the corresponding red-shifted positive excited-state absorption signal is visible for only the lower-frequency band. The diagonal signals are slightly tilted along the diagonal because of an inhomogeneous frequency distribution. However, the tilt is modest, in particular for the lower-frequency band, indicating strong homogeneous broadening contributions. The diagonal signal intensities decrease with time as a result of vibrational relaxation of the first excited state. In Figure 4a, we show this decay for the magic-angle data of the lower-frequency diagonal peak. Both

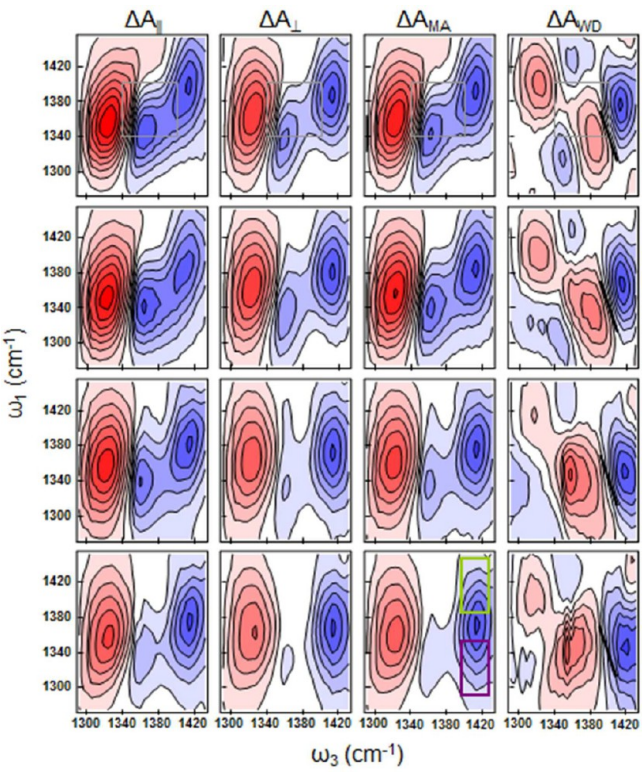

Figure 3. 2D-IR spectra of NO_3^-(aq) at different waiting times t_2 = 0, 100, 300, and 500 fs (from top to bottom). The first and second columns show spectra recorded with parallel ($\Delta A_{\parallel}$) and perpendicular ($\Delta A_{\perp}$) polarizations, respectively, of the pump and probe pulses. The third column represents the magic-angle signals ($\Delta A_{MA} = \Delta A_{\parallel} + 2\Delta A_{\perp}$). In the right column, the diagonal signals are suppressed to highlight the cross peaks in the weighted difference spectra ($\Delta A_{WD} = \kappa\Delta A_{\perp} - \Delta A_{\parallel}$) with κ = 3 (0 fs), 2.48 fs (100 fs), 1.8 (300 fs), and 1.6 (500 fs). The vertical axis is the excitation frequency, and the horizontal axis is the probe pulse frequency. Negative signals (bleach and stimulated emission) are blue, whereas positive signals (excited-state absorption) are red. All spectra are normalized to the minimum negative signal for better comparison. For better orientation, the corners of the gray squares in the first row show the centers of the diagonal and off-diagonal signals. Black lines in the last row indicate the tilt (nodal line between bleach and excited-state absorption) of the bottom right cross peak at short delays. The green and purple rectangles are the spectral regions used to calculate the signal for Figure 4c.

the bleach/stimulated-emission and the excited-state absorption signals decrease exponentially with a time constant of 550 fs.

Having established the vibrational relaxation time of the asymmetric stretch, we turn to the anisotropy of the 2D-IR spectra. Visual inspection of the first two columns of Figure 3 reveals a clear distinction between the data recorded with parallel and perpendicular pump and probe pulse polarizations. Hence, the transient absorption data are anisotropic. In Figure 4b, we plot the anisotropy $R(t)$, defined by

$$R(t) = \frac{\Delta A_{\parallel} - \Delta A_{\perp}}{\Delta A_{\parallel} + 2\Delta A_{\perp}} \quad (1)$$

for the excited-state absorption component of the lower-frequency diagonal signal of the 2D-IR spectra. It very quickly decreases from $R(0) \approx 0.4$ to $R(1\ ps) \approx 0.1$, compatible with an exponential decay with a 300-fs time constant. The residual anisotropy subsequently decays on a much slower time scale

dx.doi.org/10.1021/jp310090u | J. Phys. Chem. B 2013, 117, 3376−3388

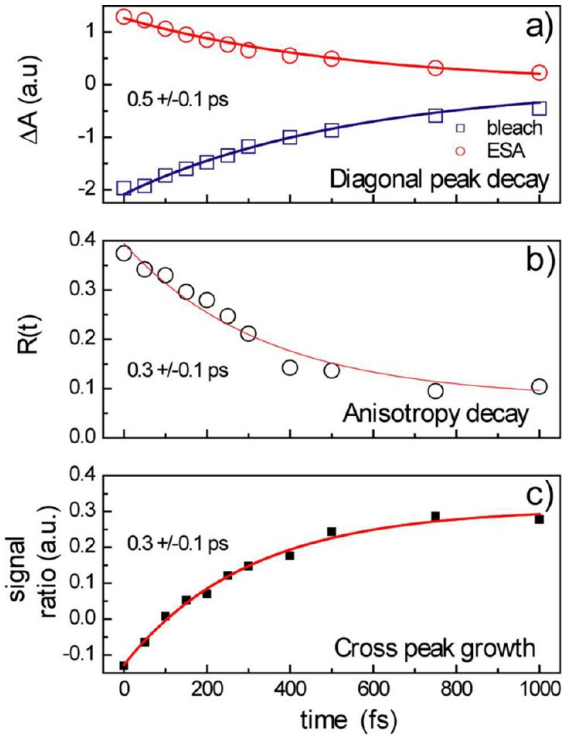

Figure 4. (a) Magic-angle signal of the lower-frequency diagonal peak at ω_1 = 1340 cm^{-1} and ω_3 = 1320 cm^{-1} (red circles, excited-state absorption component) and 1360 cm^{-1} (blue squares, ground-state bleach/stimulated emission component). Lines show single-exponential fits with a time constant of 550 fs. (b) Anisotropy decay of the lower-frequency diagonal peak (at ω_1 = 1340 cm^{-1}, ω_3 = 1320 cm^{-1}) with an exponential fit with a 300-fs time constant. (c) Cross-peak growth given by $(s_1 - s_2)/s_2$, where s_1 and s_2 are the magic-angle 2D-IR signals integrated in the spectral regions marked by the green and purple rectangles, respectively, in Figure 3. The solid line is an exponential fit with a 300-fs time constant.

that is not fully captured by the 2D-IR experiments, because the scattering background begins to dominate the signal at delays much longer than the vibrational lifetime. At t = 0, the diagonal-peak anisotropy approaches the theoretical maximum (R = 0.4) for nondegenerate transitions, for which $R(t) = {}^2/_5 P_2(\cos\theta)$. Here, P_2 is the second-order Legendre polynomial, and θ is the angle between the excited and probed transition dipole moments.

The difference between the spectra recorded with parallel and perpendicular pump and probe pulse polarizations also points to the presence of cross peaks near the off-diagonal corners of the gray squares in the first row of Figure 3 (ω_1 = 1340 cm^{-1} and ω_3 = 1400 cm^{-1}; ω_1 = 1400 cm^{-1} and ω_3 = 1340 cm^{-1}). They are partially hidden under the dominant diagonal peaks. At zero waiting time, these cross peaks indicate a coupling of the two asymmetric-stretch vibrations. Subsequently, with increasing waiting time between excitation and probing, these cross-peak signals gain relative strength with respect to the diagonal peaks. To extract the underlying kinetics, we integrated the magic-angle 2D-IR spectra in two regions with relatively little spectral overlap near ω_3 = 1420 cm^{-1}. These are marked by green and purple rectangles in the spectrum recorded after 500 fs in the third column of Figure 3 (bottom). The normalized difference of these two signals is a good approximation for the relative growth of the cross peaks on the background of the overall signal decay.[38] It is plotted in Figure 4c and can be fitted by a single-exponential function with a 300-fs rise time, which is indistinguishable from the anisotropy decay time of the diagonal peaks. A more precise determination of the kinetic time constants requires the fitting of the full 2D-IR spectra. Because of the strong correlation between the two asymmetric-stretch frequencies, established fitting procedures[39] would, however, also provide only an approximation.

To isolate the cross peaks, the dominant diagonal contributions can be eliminated by computing weighted-difference 2D-IR spectra[40] ($\Delta A_{WD} = \kappa\Delta A_\perp - \Delta A_\parallel$), using $\kappa = [1 - R(t)]/[1 + R(t)]$, where $R(t)$ is the diagonal-peak anisotropy. These difference spectra are shown in the rightmost column of Figure 3. The solid black lines reproduce the nodal line between the bleach and excited-state absorption components of the lower right off-diagonal signal at zero waiting time. It is tilted toward the antidiagonal, pointing to an anticorrelation of the frequencies of the two asymmetric-stretch modes. The antidiagonal tilt of the cross peaks can still be seen in the 300-fs spectrum, but it has decayed after about 500 fs. Because of the uncertainties in subtracting parallel and perpendicular spectra, a more quantitative analysis of the tilting angles is not possible. However, the upper left off-diagonal signals appears to be less tilted, which could indicate different broadening of the two asymmetric-stretch transitions.

UV Pump–IR Probe Spectroscopy. We now address the reorientation dynamics of NO_3^-(aq) by UV–IR transient absorption spectroscopy, which complements the 2D-IR results on the picosecond time scale. In the UV pump–IR probe measurements, the rotational anisotropy measurements are initiated by exciting the π–π^* transition of the NO_3^- ions with linearly polarized laser pulses having a wavelength of 200 nm and a duration of 200 fs. Previous studies have shown that excitation of nitrate at 200 nm leads to partial photodissociation, while approximately half of the excited nitrate molecules return to the electronic ground state and relax to the vibrational ground state.[41] The photoproducts are irrelevant to the present work. Because the transition dipole moment of the π–π^* excitation lies in the plane of the ions ($X^1A_1' \rightarrow {}^1E'$ in D_{3h} symmetry),[42] the plane of the unexcited nitrate ions remaining in the electronic ground state is predominantly perpendicular to the polarization of the excitation pulse. With time, molecular reorientation results in an isotropic distribution of the molecular planes. This reorientation was monitored by probing the asymmetric-stretch transition of NO_3^- with 100-fs linearly polarized infrared laser pulses covering the entire absorption band of the asymmetric-stretch vibration. The rotational anisotropy was derived from eq 1 by probing the induced change in the absorption measured with the probe polarization parallel ($\Delta A_\parallel$) and perpendicular ($\Delta A_\perp$) to the pump pulse polarization. Because the transition dipole moments pertaining to the π–π^* transition and the asymmetric-stretch transitions both lie in the plane of the ions, only out-of-plane molecular rotations contribute to $R(t)$. The amplitude of $R(t)$ is therefore a measure of the fraction of out-of-plane rotations relative to in-plane rotations and has a maximum theoretical value of R = 0.1. Key to applying this experimental approach to elucidate the hydrated-ion dynamics is that it selectively measures the rotation of electronic ground-state NO_3^-(aq) ions, which are *unaffected* by the excitation pulse. That is, it measures the reorientation of NO_3^- in thermal equilibrium with the bulk water network.

dx.doi.org/10.1021/jp310090u | J. Phys. Chem. B 2013, 117, 3376–3388

The time-dependent photoinduced change in the infrared absorption, $\Delta A(\nu,t)$, pertaining to the asymmetric-stretch vibration of the aqueous nitrate solution is depicted in the contour plot in Figure 5. The data set was recorded with the

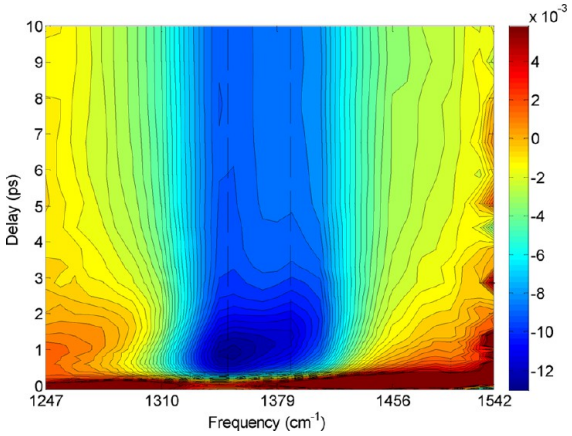

Figure 5. Contour plot of the time-dependent change in the infrared absorption $\Delta A(\nu,t)$ of the aqueous nitrate solution induced by 200-nm pump pulses. Blue indicates negative changes in the induced absorption, whereas red and yellow represent positive absorption changes. The data were recorded with the pump beam polarization parallel to the probe polarization. The dashed lines indicate the two local absorption minima associated with ground-state nitrate.

pump beam polarization parallel to the probe polarization. A similar data set was recorded with perpendicular pump and probe beam polarizations (not shown). The absorption dynamics were described in detail in a previous publication[43] and are only summarized here to explain how the reorientation dynamics were extracted from the data. The transient absorption data are dominated by a strong negative absorption change (blue) with minima at 1340 and 1400 cm^{-1} reflecting the asymmetric-stretch absorption band in Figure 1. The negative absorption change is caused by pump-induced depletion of the ground-state nitrate population. The absorption partially recovers as half of the excited nitrate ions return to the ground state during the first 10 ps. The vibrational relaxation of the nitrate ions associated with their return to the ground state is seen as the positive induced absorption (red and yellow) on the low-frequency side of the asymmetric-stretch absorption band. Because of the anharmonic ground-state potential of nitrate, this induced absorption propagates toward higher frequencies as the excited molecules relax to the vibrational ground state in 2−3 ps. The induced absorption pertaining directly to the nitrate ion is superimposed on a background covering the entire spectrum. At low frequencies, the initial dynamics of the background is obscured by the absorption associated with vibrationally relaxing nitrate molecules, whereas the transient absorption signal at high frequencies reveals an induced absorption decaying on a 2-ps time scale. A similar absorption background was observed in previous photolysis experiments on aqueous nitrite and shown to replicate the absorption change observed when the hydrogen bonds were weakened by heating the nitrite solution.[44] Accordingly, we ascribe the absorption background observed in aqueous nitrate to heated water molecules in the vicinity of the photoexcitation site.

An accurate analysis of the reorientation dynamics of the nitrate ions necessitates the separation of the absorption dynamics of ground-state nitrate ions from the absorption of vibrationally excited nitrate ions and the thermally induced absorption changes of water. In this work, this was done by singular value decomposition (SVD) of the data set. Despite the fact that the time scales for the absorptions of the three contributions are similar, SVD convincingly separates three components. The weighted spectra of the three dominating components are depicted in Figure 6a−c. The two curves in each figure represent the data obtained with the pump beam polarization parallel and perpendicular to the probe beam polarization.

Together, the three components derived by SVD account for 97% of the measured transient absorption dynamics, thus giving a nearly complete description of the data. Several important conclusions can be inferred from this analysis. The spectral component shown in Figure 6a dominates the contributions shown in Figure 6b,c by an order of magnitude. The shapes of the SVD spectra in Figure 6a derived from the measurements obtained with the two different polarizations are identical, but the (absolute) amplitude of the spectrum associated with parallel pump and probe beam polarizations is slightly larger than that obtained for perpendicular pump and probe polarizations. This is distinctly different from the spectra of the minor contributors depicted in Figure 6b,c, for which both the shapes and amplitudes of the spectra obtained for different pump and probe polarizations are identical. Accordingly, only the dominating spectral component is anisotropic. Because the time dependence of each SVD component is inherently the same at each frequency and the two minor SVD components are isotropic, the anisotropy is frequency-independent.

In general, the spectra derived by SVD represent the orthonormal basis of the spectral components rather than the spectra of the molecular species themselves. Nevertheless, comparing the dominating SVD component to the asymmetric-stretch absorption band (see Figure 6d) reveals a close similarity between the two spectra. The similarity agrees with the fact that the (negative) transient absorption resulting from photoinduced depletion of ground-state nitrate ions dominates the data in Figure 5. Hence, the dominating SVD spectrum is assigned to ground-state nitrate ions and is used as such in the following derivation of the rotational anisotropy of the aqueous nitrate ions. The assignment of the spectra in Figure 6b,c is less certain. Guided by the red shift of the absorption relative the spectrum of ground-state hydrated nitrate, the spectrum in Figure 6b might reflect the absorption associated with vibrationally relaxing nitrate molecules, while the spectrum in Figure 6c is tentatively ascribed to absorption changes induced by the local temperature increase in the sample when the NO_3^- ions were excited at 200 nm. The SVD analysis shown in Figure 6 was performed on delays between 0.5 and 44 ps. Still, the SVD analysis was rather insensitive to the chosen time interval. Thus, the SVD results remained virtually unaffected when the time interval for the analysis was changed from 0.5−5 to 0.5−44 ps. Only when using a time interval as short as 0.5−2 ps did we observe a slight change in the spectral component assigned to vibrationally relaxing nitrate ion. This change is to be expected, as the spectrum of vibrationally relaxing nitrate changes within the first 2 ps.

The rotational anisotropy, $R(t)$, was calculated by inserting the two polarization components of the SVD data assigned to the induced change in nitrate's ground-state absorption into eq 1. To improve the statistics, $R(t)$ was averaged over all probe frequencies (remember, the anisotropy is frequency-independ-

dx.doi.org/10.1021/jp310090u | J. Phys. Chem. B 2013, 117, 3376−3388

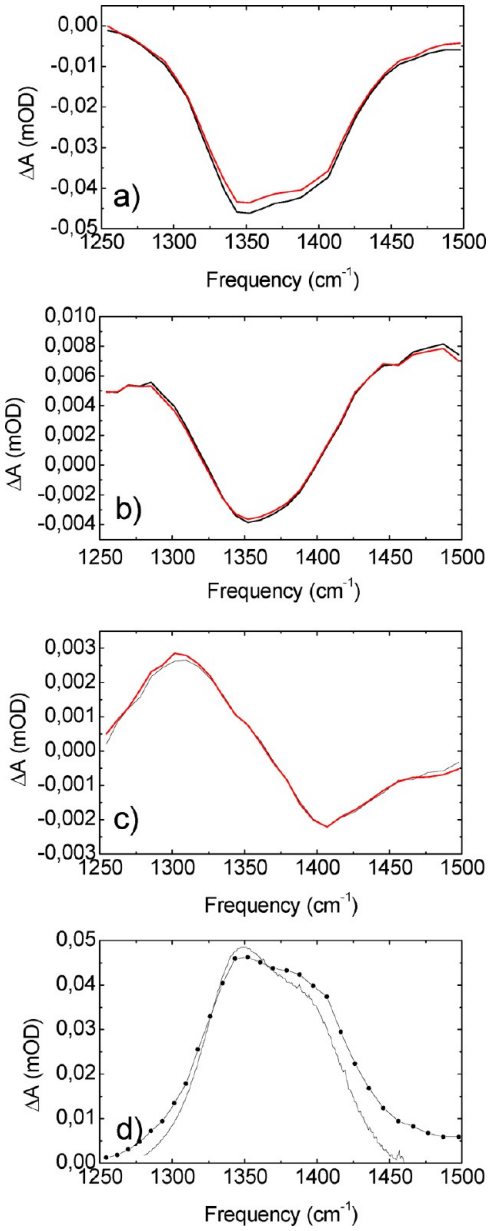

Figure 6. (a–c) Spectra of the three dominating components from the SVD analysis of the measured transient absorption dynamics presented in Figure 5. Note the different scales on the vertical axes. The component depicted in panel a is an order of magnitude large than the components in panels b and c. The two curves in each plot represent the data obtained with the pump beam polarization parallel (black) and perpendicular (red) to the probe beam polarization. Only the curves in panel a exhibit anisotropy. (d) Comparison of the dominant component in panel a (points) to the measured steady-state FTIR spectrum of ground-state nitrate (line).

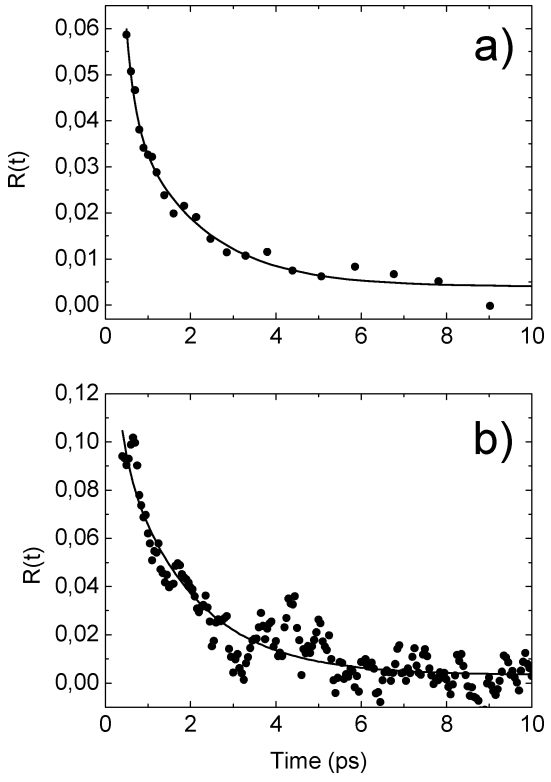

Figure 7. (a) Rotational anisotropy, $R(t)$, derived from the SVD analysis of the UV pump–IR probe transient absorption data. (b) Rotational anisotropy measured at 195 nm when aqueous nitrate was excited at 200 nm in the UV pump–UV probe measurements. Both data sets were fitted with a single-exponential function with a time constant of 1.7 ± 0.3 ps convoluted with the experimental response time (line).

ent). The resulting rotational anisotropy data presented in Figure 7a are well approximated by a single-exponential decay convoluted with the experimental response time. The initial anisotropy is $R(t = 0) = 0.05 \pm 0.01$, and the decay time is $\tau = 1.7 \pm 0.3$ ps. The initial anisotropy of $R(t = 0) = 0.05 \pm 0.01$ is somewhat lower than the maximum value of $R = 0.1$ expected for the applied pump–probe geometry. The origin of this discrepancy is unclear, but might be due to minor inaccuracies of the SVD analysis. The polarization-sensitive UV pump–UV probe transient absorption measurements presented next confirm the $\tau = 1.7 \pm 0.3$ ps reorientation time.

UV Pump–UV Probe Spectroscopy. The UV pump–UV probe rotational anisotropy measurements were initiated by exciting the π–π^* transition of the NO_3^- ions with linearly polarized laser pulses having a wavelength of 200 nm. The subsequent 195-nm probe pulses addressed the same π–π^* transition and measured the reorientation of the nitrate molecules remaining in the ground state as they relaxed to an isotropic distribution. Because the transition dipole moments pertaining to the π–π^* transition lie in the plane of the ions, only out-of-plane molecular rotations contribute to $R(t)$ in this case. As for the UV pump–IR probe measurements, the amplitude of $R(t)$ has a theoretical maximum value of $R = 0.1$. Figure 7b shows the rotational anisotropy measured at 195 nm following the excitation of hydrated nitrate ion at 200 nm. The measured anisotropy is well approximated by a single-exponential decaying function having an initial value of $R(t = 0) = 0.1 \pm 0.01$ and a time constant of $\tau = 1.7 \pm 0.3$ ps. This reorientation time is in full agreement with the $\tau = 1.7 \pm 0.3$ ps derived from the UV pump–IR probe measurements and furthermore agrees with the 2 ± 0.2 ps rotation time derived from line-width analysis of Raman spectra of aqueous nitrate by Perelygin et al.[22] Consequently, there is compelling experimental evidence that the hydrated nitrate ions perform out-of-plane rotations on a 2-ps time scale. The initial value of the rotational anisotropy of $R(t = 0) = 0.1$ agrees with the

dx.doi.org/10.1021/jp310090u | J. Phys. Chem. B 2013, 117, 3376–3388

theoretical maximum value expected for molecules with transition dipole moments defining a plane.

MD Simulations. Classical MD and CPMD simulations were carried out to obtain information about the reorientation of the vibrational transition dipole moments for direct comparison with the experimental data. Because aqueous nitrate has already been the subject of a number of MD and quantum mechanics/molecular mechanics (QM/MM) simulations, we begin with a discussion of the solvation structure around the solute to motivate our approach. In Figure 8, the radial distribution functions (RDFs) of the atoms in nitrate (N, O) and the atoms in water (O_w, H_w) are presented.

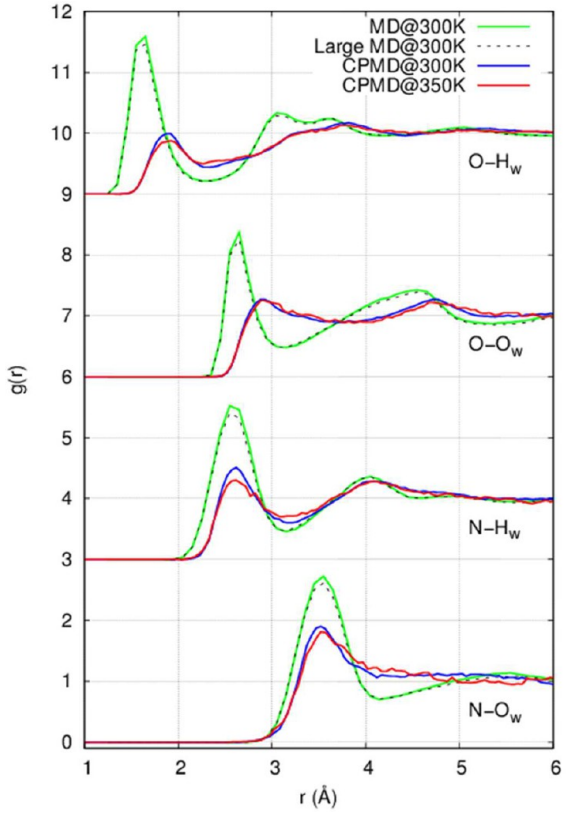

Figure 8. Radial distribution functions for the solvation structure around nitrate: results from classical MD simulations with either 55 (green lines) or 550 (dashed lines) water molecules compared with results from CPMD simulations at 300 K (blue lines) and 350 K (red lines).

The size dependence of the solvation structure in the classical MD simulation is weak, and there is only a moderate temperature dependence in the CPMD simulations. However, the hydration shell of NO_3^- is much less structured in the CPMD simulations than in the classical MD simulations. In CPMD, the structure of the hydration shell around NO_3^- is weak, with rapid fluctuations in the hydrogen-bond network. This is in qualitative agreement with earlier ab initio quantum mechanical charge-field MD studies.[35,45] For the N−O_w and O−O_w RDFs, there is good agreement between our CPMD results and previous QM/MM results[45] obtained with the QM-B3LYP approximation. However, there are significant differences between the CPMD and QM/MM methods for the RDFs involving H_w and in the water structure outside the first hydration shell. The consistent force field in CPMD provides a balanced description of solvent and solute, but it is known to predict a too-structured hydrogen-bond network in water. However, the local structure in the hydration of the nitrate ions predicted by CPMD is in agreement with QM/MM and deemed more trustworthy than that obtained by classical MD. Our classical MD simulations were based on a standard point-charge model, which clearly gives an overly strong hydration of the nitrate ion. In a follow-up study, we will analyze the structure and dynamics of prolonged CPMD simulations for comparison to other MD force fields, including that derived in the QM/MM study.[45]

We also compared the reorientational dynamics between the CPMD and classical MD simulations. Figure 9 presents the

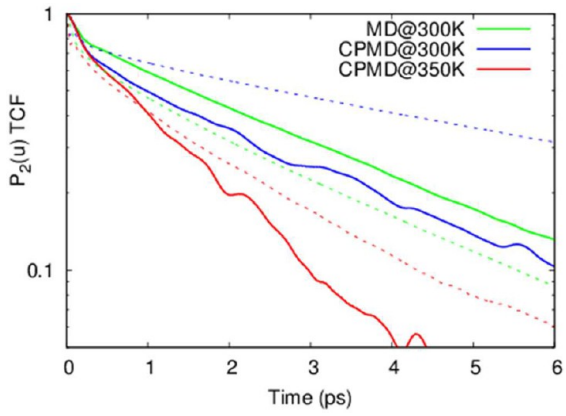

Figure 9. Reorientational motions of nitrate (solid lines) and water (dashed lines) in terms of the time correlation functions (TFCs) for the second-order Legendre polynomial, $P_2(u)$, of the N−O vector and the O−H vector in water: results from classical MD simulation (green lines) compared with results from CPMD simulations at 300 K (blue lines) and 350 K (red lines).

time-correlation function (TCFs) of the second-order Legendre polynomial, $\langle P_2[u(t_0 + t)\cdot u(t_0)]\rangle \sim R(t)$ (eq 1), of the N−O vector in the nitrate ion and that of O−H vectors in the water molecules. Time scales for the reorientation processes were derived by fitting the TCFs in Figure 9 to single-exponential decays in the interval 1−4 ps. In the classical simulation, the $P_2(u)$ TCF shows that orientational motion of the nitrate ion (τ = 3.225 ± 0.005 ps) is slower than that of the water molecules (τ = 2.794 ± 0.005 ps). In CPMD, however, the relationship is reversed at both temperatures, and the water molecules undergo very slow reorientation at 300 K. Thus, for the CPMD simulations at 300 K (350 K), the time constant of the correlation function of the nitrate ion is τ = 3.1 ± 0.2 ps (τ = 1.5 ± 0.2 ps), and that for the water molecules is τ = 6.71 ± 0.05 ps (τ = 2.30 ± 0.05 ps). The uncertainty of the correlation times of nitrate from the CPMD simulation is largely due to the limited sampling. A ratio of 2 between the correlation times of nitrate and water is significant and too large to be explained by the deuteration used in the CPMD simulations. In comparisons to the experimental results, it is important to remember that quantum effects strongly affect the reorientational correlations time in water.[46] The slow dynamics in CPMD simulations is usually handled by an ad hoc temperature increase, which is why we also performed a CPMD simulation at 350 K.

For comparison to the vibrational probes, we calculated harmonic frequencies in quantum chemical calculations on clusters cut from the periodic simulation models. A full

dx.doi.org/10.1021/jp310090u | J. Phys. Chem. B 2013, 117, 3376−3388

theoretical treatment of the nonlinear spectroscopy would require a quantum mechanical treatment involving overtones[21] and very expensive long trajectories. However, because our objective was to identify the relation between the molecular interactions and the spectral response, we simply sampled static spectra over the MD trajectories. Although the present CPMD simulation was too short for the calculation of accurate correlation functions, the sampling was sufficient to obtain a qualitative picture of the mechanism for the 2D-IR experiment. The absorption bands of the stretching modes were calculated by sampling static vibrational spectra over configurations along the MD trajectory. The spectrum resulting from the CPMD simulation, shown in Figure 10a satisfactorily reproduced the

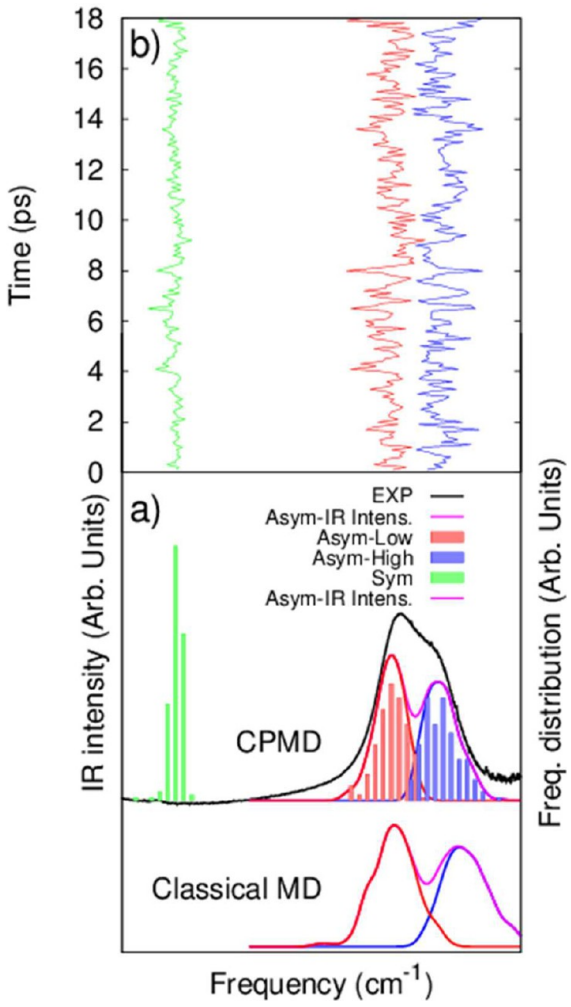

Figure 10. (a) Calculated absorption spectrum of the asymmetric stretch extracted from the MD simulations. The calculated spectrum is compared to the experimentally determined absorption spectrum of Figure 1. Frequency distributions are displayed as bar diagrams, without considering transition strengths. A simulated spectrum based on classical MD is also included. (b) Instantaneous frequencies as a function of time.

frequency, as well as the width and frequency splitting, of the experimental asymmetric-stretch band. In the lower part of Figure 8a, a similar analysis of the configurations in the classical MD simulation revealed a splitting that was overestimated. Accordingly, the differences in the solvation structure noticed in the RDFs in Figure 8 around the nitrate ion are reflected in the IR spectra. This shows that the combination of the reorientation dynamics and the IR spectrum gives constraints on the solvation of the nitrate ion. Figure 10b shows the instantaneous frequencies as a function of time. In agreement with the 2D-IR data, there is a clear anticorrelation between the high and low frequencies in the sampled asymmetric stretches. For the same configuration, a strong red shift in one of the asymmetric stretches is associated with a reduced red shift in the other stretching frequency. The distribution of the symmetric-stretch frequency is narrower, but the variations are also correlated with the asymmetric-stretch modes. The variations in frequency are related to the hydration of the N−O groups. Hence, we can use the splitting to characterize the degree of asymmetry in the hydration shell.

Figure 11a shows the orientation of the transition dipole moment relative to a given N−O bond for the high- and low-

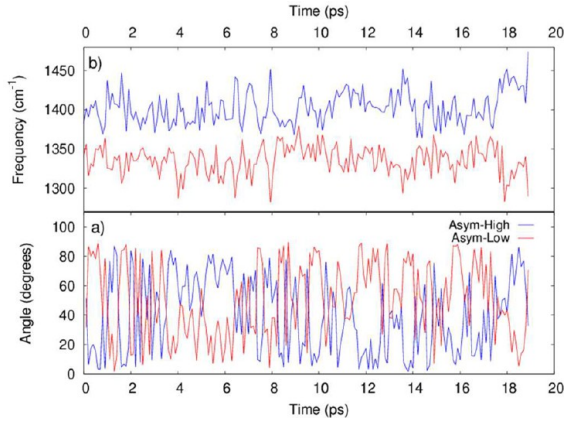

Figure 11. (a) Time-dependent orientation of the asymmetric-stretch transition dipole moments (modeled as dipole derivatives of the vibrational modes) relative to a N−O bond direction in a molecule-fixed frame. Red and blue colors indicate lower- and higher-frequency transitions, respectively. (b) Frequency fluctuations in the asymmetric-stretch modes presented in Figure 10b plotted again to highlight the correlation with the reorientational dynamics in panel a.

frequency components of the asymmetric-stretch absorption band. In the graph, one can follow how the angle between a given N−O vector and the transition moments changes on a subpicosecond time scale. The Car−Parrinello MD simulations also reveal how the frequency fluctuations of the asymmetric-stretch vibrations correlate with the reorientations of the vibrational transition moment. The weak correlation between the angular changes in Figure 11a and the frequency fluctuations in Figure 10b suggests that the angular jumps occur predominantly when the frequency splitting is small, that is, when the solvation shell is nearly symmetric. This indicates that the anisotropy decay observed in 2D-IR experiments with a time constant of 300 fs can be related to reorientations of the transition dipole moments, which do not require the physical rotation of the NO_3^- anion in the laboratory frame. Hence, we refer to these dynamics as pseudorotations in the molecular frame.

DISCUSSION

To summarize the results, the reorientation of NO_3^- in water was investigated by three complementary ultrafast spectroscopic probes. In the all-infrared 2D-IR experiments, we both excited and probed the asymmetric-stretch transition dipoles.

dx.doi.org/10.1021/jp310090u | J. Phys. Chem. B 2013, 117, 3376−3388

The initial anisotropy close to 0.4 is a signature of a nondegenerate transition and directly confirms that the degeneracy of the asymmetric-stretch vibration of the molecule is lifted in aqueous solution. As a result, both in-plane and out-of-plane reorientations can be detected. Within the first few hundred femtoseconds after excitation, the transition dipole moments of the asymmetric-stretch vibrations partially lose the memory of their original orientation. The anisotropy decays to a residual value of 0.1, characteristic of a plane-degenerate transition. Consistent with this observation, the CPMD simulations report a large number of orientation flips within a few picoseconds of the IR transition dipole moments in the molecular frame (see Figure 11). Accordingly, the 300-fs time constant in our experiments should be assigned to an in-plane pseudorotation of the transition dipole moments that does not require the reorientation of the ion itself. Physical reorientation (tumbling of the molecular plane) takes picoseconds. This motion was probed by the anisotropy decay in the UV−UV and UV−IR experiments, where we excited a plane-polarized electronic transition, so that the measurements were sensitive only to the reorientation of the molecular plane. We thus confirmed an earlier analysis of the symmetric-stretch Raman band of nitrate,[22] which produced a remarkably similar time constant (2 ± 0.3 ps).

The fast anisotropy decay of the diagonal peaks in the 2D-IR spectrum takes place on the same time scale as the redistribution of vibrational excitation between the two asymmetric-stretch modes of NO_3^-(aq), which can be monitored by the relative growth of the cross-peak signals with a 300-fs time constant (Figures 3 and 4). Usually, for nondegenerate transitions, the transfer of excitation from one vibrational mode to another does not lead to a significant reorientation of the corresponding transition dipole moments. In fact, the anisotropy of cross peaks arising from excitation transfer can often even be used to obtain information on molecular structure.[47] For a plane-degenerate excited state, on the other hand, coherent linear combinations of the two transitions can be excited, which can lead to initial anisotropy values different from 0.4.[48,49] Anisotropy decay to a value of 0.1 is then a signature of the formation of a statistical mixture of the two transitions after dephasing.[50]

Aqueous nitrate is an intermediate case, where the solvent-induced splitting of the two asymmetric-stretch transitions is sufficiently strong to produce two separate absorption bands. The 2D spectra also separate the diagonal- and cross-peak contributions, which overlap and can cause unusual anisotropy values in conventional pump−probe data. Despite the clear distinction between excitation and probing of lower- and higher-frequency modes in our experiments, we observed in-plane randomization of the transition dipole moment orientations on an ultrafast time scale. Excitation transfer alone, as observed for example, between different water molecules with overlapping OH stretch spectra,[51] is not sufficient to account for this observation. For illustration, consider the schematic picture of solvated nitrate ions in Figure 12. The splitting of the asymmetric-stretch band in Figure 12a arises from the elongation of one N−O bond due to (stronger) hydrogen bonding, essentially stabilizing one of the resonance structures of NO_3^-. The corresponding transition dipole moments are then oriented in the molecular frame as indicated by the blue (higher-frequency) and red (lower-frequency) solid arrows. In this configuration, transfer of excitation from one asymmetric-stretch mode to the other would lead to cross-peak

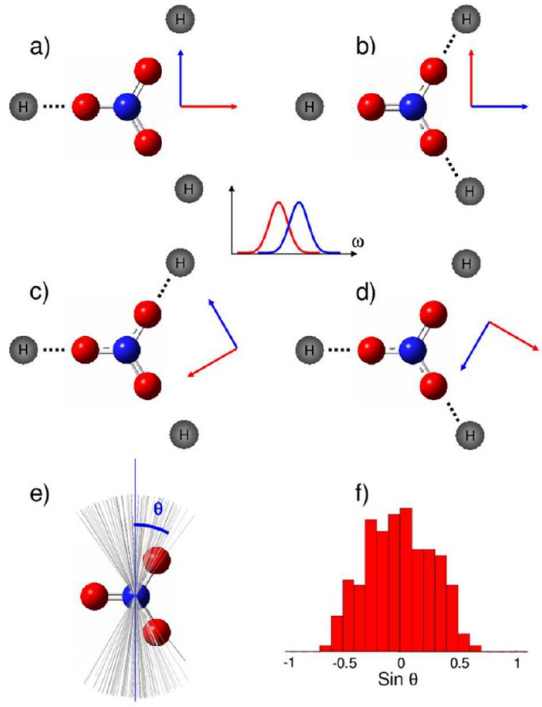

Figure 12. (a−d) Schematic representation of different solvated ion configurations. Transitions between these configurations caused by solvation-shell fluctuations can explain the observed cross-peak growth and simultaneous decay of the diagonal-peak anisotropy due to reorientation of their transition dipole moments. Dipole moment orientations are indicated by red and blue arrows, which correspond to lower- and higher-frequency transitions, respectively. (e) Transition dipole orientations of the lower-frequency asymmetric-stretch transition from our sampling of the CPMD simulation in the molecular frame after aligning all molecules along the shortest N−O bond, pointing in the x direction. (f) Histogram of the angle distribution.

growth and diagonal-peak decay, but it would not affect the anisotropy of the diagonal peaks. The same is true for the configuration sketched in Figure 12b, in which one nitrogen atom is more weakly hydrogen bonded than the other two. Fluctuations of the hydration shell, on the other hand, can rapidly stabilize different "resonance structures" of the nitrate ion, leading to a reorientation (Figure 12c,d) of the transition dipole moments, or there could even be an exchange of frequency ordering (transition between the configurations in panels a and b). As the normal-mode coordinates change, the initial excitation is projected onto a new basis. Population redistribution and anisotropy decay thus have a common cause and take place concomitantly.

In a recent study of guanidinium in water and water−glycerol mixtures, Vorobyev et al. analyzed in detail the effects of excitation versus energy transfer on the anisotropy of 2D-IR and dispersed photon-echo signals of a quasidegenerate mode.[23] They concluded that, in their case, fast anisotropy decay was primarily caused by excitation transfer, whereas reorientation of the transition dipole moments was slower. For guanidinium, however, a weak band splitting that allows one to distinguish cross-peak and diagonal-peak contributions can be observed only in water−glycerol mixtures but not in pure water. It is thus possible that the interaction with glycerol stabilizes an asymmetric charge distributions in guanidinium for a longer time than water can support a given hydration shell around

dx.doi.org/10.1021/jp310090u | J. Phys. Chem. B 2013, 117, 3376−3388

nitrate. The 2D-IR model spectra presented in ref 23, on the other hand, clearly illustrate that the diagonal-peak anisotropy cannot decay by excitation transfer alone.

Note that transitions between configurations such as those shown in Figure 12 require only modest changes in the strength of the hydrogen bonds between water molecules and the ion. Indeed, previous MD simulations of the structural dynamics of nitrate's hydration shell already showed a substantial asymmetry in both the structure and dynamics of the hydrogen bonds.[35] This asymmetry is correlated with transient elongations of individual N−O bonds associated with charge redistribution in the NO_3^- ion.[36] The charge redistribution dynamics is accompanied by rapid (0.2−0.9-ps) fluctuations of the hydrogen bonds. In our Car−Parrinello simulations, we found that the lower-frequency asymmetric-stretch transition dipole moment was always confined to an angle section of approximately ±30° perpendicular to the shortest N−O bond, as shown in Figure 12e,f. The idealized configurations in Figure 12b−d can be regarded as a qualitative representation of this result. Aligning all computed NO_3^- structures along the longest N−O bond yields a somewhat wider distribution of transition dipole angles (not shown). A single long intramolecular bond as sketched in Figure 12a thus seems to be less frequent. Indeed, most structures are characterized by three distinct bond lengths, leading to the observed distribution of angles. The N−O bond length reflects the strength of hydrogen bonding to that N−O group. Hence, in terms of solvation, the observed asymmetry means that the situation with enhanced hydrogen bonding at two of the N−O groups is more frequent than that of a single N−O group being strongly hydrogen bonded. Hence, the distribution of transition moments taken along the shortest N−O bond will be narrower than the distribution along either of the longer bonds. For reorientation within the cone in Figure 12f, the longer two bonds exchange their roles, whereas the large jumps in transition dipole orientation seen in Figure 11 are always accompanied by the lengthening of the formerly shortest N−O bond and the shortening of a previously longer bond. These jumps can therefore be associated with charge redistribution in the ion as a result of changes in the structure of the hydration shell. The anisotropy decay and excitation transfer in the 2D-IR spectra of the asymmetric-stretch vibrations thus directly report on the time scale of hydrogen-bond fluctuations between water and the ion.

In a systematic analysis of nitrate's asymmetric-stretch band, Ramesh et al.[21] treated the ion−bath interaction as forces in normal-mode coordinates of undistorted NO_3^-. Already when restricting the calculations to only the two antisymmetric-stretch vibrations, it was possible to reproduce the observed band splitting. [Their parameters for a two-dimensional potential can even be "abused" to predict a ratio of diagonal/off-diagonal anharmonicities (3:1) that is in qualitative agreement with the ratio of diagonal- to cross-peak intensities in our 2D-IR spectra.] Other normal modes, in particular force components along the symmetric-stretch coordinate, needed to be included in the analysis to quantitatively match the shape and asymmetry of the experimental spectrum.[21] Consideration of only the asymmetric-stretch vibrations necessarily results in a perfect anticorrelation of the two asymmetric-stretch frequencies. Force fluctuations along the symmetric-stretch coordinate, on the other hand, seem to be mainly responsible for (inhomogeneous) broadening and tend to shift both asymmetric-stretch transitions. Indeed, the small tilt of the cross peaks in our 2D-IR spectra indicate only a relatively weak anticorrelation, in agreement with the frequency trajectories of our CPMD simulations. Further reduction of the tilt of diagonal and cross peaks is certainly due to homogeneous broadening contributions. These can arise not only from fast frequency fluctuations, but also directly from the rapid reorientation of the transition dipole moments. Because of this complexity, the detailed analysis of the 2D-IR line shapes is left for future work. Here, we have concentrated on the direct implications of our observations for our picture of the water−ion interactions. On the 300-fs time scale discussed so far, nitrate does not rotate, as the time constant of rotational diffusion in the UV−IR and UV−UV measurements is approximately 2 ps. Hence, the hydrogen bonds fluctuate several times before the ion reorients. It is unlikely that reorientation with a 2-ps time constant is possible without an exchange of hydrogen-bonding partners, so nitrate cannot be dragging a longer-lived hydration shell. The CPMD simulations confirm that hydrogen bonds are indeed broken and re-formed with new partners. Interestingly, very similar time constants for hydrogen-bond fluctuations of <1 ps[4,5] and rotational diffusion of 2.5 ps have been reported for isotope-labeled water.[7] Despite its negative charge, nitrate does not seem to strongly perturb its local environment. However, because NO_3^- does not distort the water spectrum in the same way as BF_4^- or ClO_4^-, for example, we cannot directly probe the reorientation of the water molecules surrounding the ion. The spectroscopy of the asymmetric-stretch vibrations and Car−Parrinello MD simulations nevertheless suggest that the hydration "shell" of nitrate is by no means a static entity—in fact, it appears to be just as labile as neat water.

In agreement with the experimental results, the CPMD simulations found that the reorientation of the nitrate ion might be faster than that of the surrounding solvent molecules. Comparison of the results from the CPMD simulations and the classical MD simulations shows that the ratio of the reorientational correlation times of solute and solvent depends on the solvation structure. In CPMD, the fast motion of the nitrate molecules is associated with a weakly structured first solvation shell.

CONCLUSIONS

In summary, the anisotropy decay in 2D-IR and transient absorption spectra of aqueous nitrate was analyzed with the help of Car−Parrinello molecular dynamics simulations. Fluctuations of the solvating water molecules provoke frequent symmetry-breaking changes in N−O bond lengths. The instantaneous normal-mode coordinates of the asymmetric-stretch vibrations, whose degeneracy is lifted by these asymmetric distortions in water, are therefore continuously changing. This was observed as a rapid reorientation of the transition dipole moments concomitant with excitation redistribution between the two asymmetric-stretch modes, revealing a 300-fs time constant. Key to the experimental distinction between mode reorientation and simple excitation hopping was the large splitting of the asymmetric-stretch band and clear distinction between diagonal- and cross-peak signals in the 2D-IR spectra. Nonlinear spectroscopy can thus clearly identify the characteristic time for hydrogen-bond fluctuations and—through the anisotropy decay of the pump−probe data—the persistence time of ion−water hydrogen bonds, which is approximately 5 times longer. As both time scales are very similar to those reported for isotope-labeled water, we inferred that the water molecules surrounding the nitrate ion do not

dx.doi.org/10.1021/jp310090u | J. Phys. Chem. B 2013, 117, 3376−3388

form a very stable hydration shell. As a consequence, the theoretical description of NO_3^-(aq) is expected to depend critically on the quality of the water model, and indeed, we found that the structural details in the vicinity of the ion differed between our CPMD results and those of previous MD and QM/MM approaches. However, the rapid reorientation of the vibrational dipole transition moments caused by symmetry-breaking fluctuations in the hydrogen-bond network around the nitrate ion is a general finding that is not specific to the CPMD simulation model but also present for the classical force field. The CPMD simulations showed that the reorientation of the nitrate anion is faster than that of the water molecules, which is an interesting result, because earlier IR studies indicated that the reorientation of water molecules is slowed in the vicinity of anions.[1,3,12,52] Insight from this study shows how these data can be reconciled. In a weakly structured solvation shell, a small anion can reorient without dragging its first solvation shell with it. Hence, the anion will rotate while the water molecules in the cage around it will remain influenced by the electrostatic field of the ion. A speculative mechanism would be that water molecules temporarily reorient when the hydrogen bond to the anion breaks, but that there is a high probability for re-forming a hydrogen bond to the same anion, although to a different oxygen atom. In future studies, we will perform detailed analysis of prolonged simulations to test this hypothesis. In this context, a comparison of CPMD with other simulation models such as ab initio QM/MM approaches and classical polarizable force fields will be interesting. Here, we used theory primarily to interpret our experimental observables, but we did not attempt to compute spectra or correlation functions for a quantitative comparison. Given the high sensitivity of the asymmetric-stretch vibrations to solvation despite the relatively weak molecular interactions, this might be a critical albeit difficult test for the ability to describe and understand the very details of hydration.

AUTHOR INFORMATION

Corresponding Author

*E-mail: thogersen@chem.au.dk (J.T.), odelius@fysik.su.se (M.O.), j.helbing@pci.uzh.ch (J.H.).

Notes

The authors declare no competing financial interest.

ACKNOWLEDGMENTS

M.O. thanks the Swedish Research Council, Carl Tryggers Foundation, and Magnus Bergvall Foundation for financial support. The MD simulations were made possible through generous allocations of computer time through SNIC at the Swedish National Supercomputer Center (NSC) and High Performance Computing Center North (HPC2N), Sweden. S.R.K. thanks the Danish Council for Independent Research and the Carslberg Foundation for financial support.

REFERENCES

(1) Marcus, Y. Effect of Ions on the Structure of Water: Structure Making and Breaking. *Chem. Rev.* **2009**, *109*, 1346−1370.

(2) Ohtaki, H.; Radnai, T. Structure and Dynamics of Hydrated Ions. *Chem. Rev.* **1993**, *93*, 1157−1204.

(3) Bakker, H. J. Structural Dynamics of Aqueous Salt Solutions. *Chem. Rev.* **2008**, *108*, 1456−1473.

(4) Eaves, J. D.; Loparo, J. J.; Fecko, C. J.; Roberts, S. T.; Tokmakoff, A.; Geissler, P. L. Hydrogen Bonds in Liquid Water Are Broken Only Fleetingly. *Proc. Natl. Acad. Sci. U.S.A.* **2005**, *102*, 13019−13022.

(5) Woutersen, S.; Emmerichs, U.; Nienhuys, H. K.; Bakker, H. J. Anomalous Temperature Dependence of Vibrational Lifetimes in Water and Ice. *Phys. Rev. Lett.* **1998**, *81*, 1106−1109.

(6) Laage, D.; Hynes, J. T. On the Molecular Mechanism of Water Reorientation. *J. Phys. Chem. B* **2008**, *112*, 14230−14242.

(7) Rezus, Y. L. A.; Bakker, H. J. On the Orientational Relaxation of HDO in Liquid Water. *J. Chem. Phys.* **2005**, *123*, 114502−114507.

(8) Laage, D.; Hynes, J. T. A Molecular Jump Mechanism of Water Reorientation. *Science* **2006**, *311*, 832−835.

(9) Laage, D.; Stirnemann, G.; Sterpone, F.; Hynes, J. T. Water Jump Reorientation: From Theoretical Prediction to Experimental Observation. *Acc. Chem. Res.* **2012**, *45*, 53−62.

(10) Laage, D. Reinterpretation of the Liquid Water Quasi-Elastic Neutron Scattering Spectra Based on a Nondiffusive Jump Reorientation Mechanism. *J. Phys. Chem. B* **2009**, *113*, 2684−2687.

(11) Ji, M.; Odelius, M.; Gaffney, K. J. Large Angular Jump Mechanism Observed for Hydrogen Bond Exchange in Aqueous Perchlorate Solution. *Science* **2010**, *328*, 1003−1005.

(12) Gaffney, K. J.; Ji, M.; Odelius, M.; Park, S.; Suna, Z. H-Bond Switching and Ligand Exchange Dynamics in Aqueous Ionic Solution. *Chem. Phys. Lett.* **2011**, *504*, 1−6.

(13) Kropman, M. F.; Bakker, H. J. Femtosecond Mid-infrared Spectroscopy of Aqueous Solvation Shells. *J. Chem. Phys.* **2001**, *115*, 8942−8948.

(14) Omta, A. W.; Kropman, M. F.; Woutersen, S.; Bakker, H. J. Negligible Effect of Ions on the Hydrogen-Bond Structure in Liquid Water. *Science* **2003**, *301*, 347−349.

(15) Tielrooij, K. J.; Garcia-Araez, N.; Bonn, M.; Bakker, H. J. Cooperativity in Ion Hydration. *Science* **2010**, *328*, 1006−1009.

(16) Laage, D.; Stirnemann, G.; Hynes, J. T. Why Water Reorientation Slows without Iceberg Formation around Hydrophobic Solutes. *J. Phys. Chem. B* **2009**, *113*, 2428−2435.

(17) Laage, D.; Stirnemann, G.; Sterpone, F.; Rey, R.; Hynes, J. T. Reorientation and Allied Dynamics in Water and Aqueous Solutions. *Annu. Rev. Phys. Chem.* **2011**, *62*, 395−416.

(18) Park, S.; Odelius, M.; Gaffney, K. J. Ultrafast Dynamics of Hydrogen Bond Exchange in Aqueous Ionic Solutions. *J. Phys. Chem. B* **2009**, *113*, 7825−7835.

(19) Moilanen, D. E.; Wong, D.; Rosenfeld, D. E.; Fenn, E. E.; Fayer, M. D. Ion−Water Hydrogen-Bond Switching Observed with 2D IR Vibrational Echo Chemical Exchange Spectroscopy. *Proc. Natl. Acad. Sci. U.S.A.* **2009**, *106*, 375−380.

(20) Timmer, R. L. A.; Bakker, H. J. Hydrogen Bond Fluctuations of the Hydration Shell of the Bromide Anion. *J. Phys. Chem. A* **2009**, *113*, 6104.

(21) Ramesh, S. G.; Re, S.; Boisson, J.; Hynes, J. T. Vibrational Symmetry Breaking of NO_3^- in Aqueous Solution: NO Asymmetric Stretch Frequency Distribution and Mean Splitting. *J. Phys. Chem. A* **2010**, *114*, 1255−1269.

(22) Perelygin, I. S.; Mikhailov, G. P.; Tuchkov, S. V. Vibrational and Orientational Relaxation of Polyatomic Anions and Ion-Molecular Hydrogen Bond in Aqueous Solutions. *J. Mol. Struct.* **1996**, *381*, 189−192.

(23) Vorobyev, D. Y.; Kuo, C.-H.; Kuroda, D. G.; Scott, J. N.; Vanderkooi, J. M.; Hochstrasser, R. M. Water-Induced Relaxation of a Degenerate Vibration of Guanidinium Using 2D IR Echo Spectroscopy. *J. Phys. Chem. B* **2010**, *114*, 2944−2953.

(24) Helbing, J.; Hamm, P. Compact Implementation of Fourier Transform Two-Dimensional IR Spectroscopy without Phase Ambiguity. *J. Opt. Soc. Am. B* **2011**, *28*, 171.

(25) Tauber, M. J.; Mathies, R. A.; Chen, X.; Bradforth, S. E. Flowing Liquid Sample Jet for Resonance Raman and Ultrafast Optical Spectroscopy. *Rev. Sci. Instrum.* **2003**, *74*, 4958−4960.

(26) Isono, T. Density, Viscosity, and Electrolytic Conductivity of Concentrated Aqueous Electrolyte Solutions at Several Temperatures. Alkaline-Earth Chlorides, Lanthanum Chloride, Sodium Chloride, Sodium Nitrate, Sodium Bromide, Potassium Nitrate, Potassium Bromide, and Cadmium Nitrate. *J. Chem. Eng. Data* **1984**, *29*, 45.

(27) Lyubartsev, A. P.; Laaksonen, A. M.Dyna*Mix*—A Scalable Portable Parallel MD Simulation Package for Arbitrary Molecular Mixtures. *Comput. Phys. Commun.* **2000**, *128*, 565−589.
(28) Jayaraman, S.; Thompson, A. P.; von Lilienfeld, O. A.; Maginn, E. Molecular Simulation of the Thermal and Transport Properties of Three Alkali Nitrate Salts. J. *Ind. Eng. Chem. Res.* **2010**, *49*, 559−571.
(29) Vchirawongkwin, V.; Sato, H.; Sakaki, S. RISM-SCF-SEDD Study on the Symmetry Breaking of Carbonate and Nitrate Anions in Aqueous Solution. *J. Phys. Chem. B* **2010**, *114*, 10513−10519.
(30) Car, R.; Parrinello, M. Unified Approach for Molecular Dynamics and Density-Functional Theory. *Phys. Rev. Lett.* **1985**, *55*, 2471.
(31) *CPMD V3.11*; IBM Corp./MPI fuer Festkoerperforschung Stuttgart, 2011.
(32) Frisch, M. J.; Trucks, G. W.; Schlegel, H. B.; Scuseria, G. E.; Robb, M. A.; Cheeseman, J. R.; Scalmani, G.; Barone, V.; Mennucci, B.; Petersson, G. A.; Nakatsuji, H.; Caricato, M.; Li, X.; Hratchian, H. P.; Izmaylov, A. F.; Bloino, J.; Zheng, G.; Sonnenberg, J. L.; Hada, M.; Ehara, M.; Toyota, K.; Fukuda, R.; Hasegawa, J.; Ishida, M.; Nakajima, T.; Honda, Y.; Kitao, O.; Nakai, H.; Vreven, T.; Montgomery, J. A., Jr.; Peralta, J. E.; Ogliaro, F.; Bearpark, M.; Heyd, J. J.; Brothers, E.; Kudin, K. N.; Staroverov, V. N.; Keith, T.; Kobayashi, R.; Normand, J.; Raghavachari, K.; Rendell, A.; Burant, J. C.; Iyengar, S. S.; Tomasi, J.; Cossi, M.; Rega, N.; Millam, J. M.; Klene, M.; Knox, J. E.; Cross, J. B.; Bakken, V.; Adamo, C.; Jaramillo, J.; Gomperts, R.; Stratmann, R. E.; Yazyev, O.; Austin, A. J.; Cammi, R.; Pomelli, C.; Ochterski, J. W.; Martin, R. L.; Morokuma, K.; Zakrzewski, V. G.; Voth, G. A.; Salvador, P.; Dannenberg, J. J.; Dapprich, S.; Daniels, A. D.; Farkas, Ö.; Foresman, J. B.; Ortiz, J. V.; Cioslowski, J.; Fox, D. J. *Gaussian 09*, revision B.01; Gaussian, Inc.: Wallingford, CT, 2010.
(33) Shen, M.; Xie, Y.; Henry F. Schaefer, I.; Deakyne, C. A. Hydrogen Bonding between the Nitrate Anion (Conventional and Peroxy Forms) and the Water Molecule. *J. Chem. Phys.* **1990**, *93*, 3379−3388.
(34) Waterland, M. R.; Stockwell, D.; Kelley, A. M. Symmetry Breaking Effects in NO_3^-: Raman Spectra of Nitrate Salts and Ab Initio Resonance Raman Spectra of Nitrate−Water Complexes. *J. Chem. Phys.* **2001**, *114*, 6249−6258.
(35) Vchirawongkwin, V.; Kritayakornupong, C.; Tongraar, A.; Rode, B. M. Symmetry Breaking and Hydration Structure of Carbonate and Nitrate in Aqueous Solutions: A Study by Ab Initio Quantum Mechanical Charge Field Molecular Dynamics. *J. Phys. Chem. B* **2011**, *115*, 12527−12536.
(36) Lebrero, M. C. G.; Bikiel, D. E.; Elola, M. D.; Estrin, D. A.; Roitberg, A. E. Solvent-Induced Symmetry Breaking of Nitrate Ion in Aqueous Clusters: A Quantum-Classical Simulation Study. *J. Chem. Phys.* **2002**, *117*, 2718−2725.
(37) Goebbert, D. J.; Garand, E.; Wende, T.; Bergmann, R.; Meijer, G.; Asmis, K. R.; Neumark, D. M. Infrared Spectroscopy of the Microhydrated Nitrate Ions $NO_3^-(H_2O)_{1-6}$. *J. Phys. Chem. A* **2009**, *113*, 7584.
(38) Woutersen, S.; Mu, Y.; Stock, G.; Hamm, P. Subpicosecond Conformational Dynamics of Small Peptides Probed by Two-Dimensional Vibrational Spectroscopy. *Proc. Natl. Acad. Sci. U.S.A.* **2001**, *98*, 11254−11258.
(39) Kwak, K.; Zheng, J.; Cang, H.; Fayer, M. D. Ultrafast Two-Dimensional Infrared Vibrational Echo Chemical Exchange Experiments and Theory. *J. Phys. Chem. B* **2006**, *110*, 19998−20013.
(40) Woutersen, S.; Hamm, P. Structure Determination of Trialanine in Water Using Polarization Sensitive Two-Dimensional Vibrational Spectroscopy. *J. Phys. Chem.* **2000**, *104*, 11316−11320.
(41) Madsen, D.; Larsen, J.; Jensen, S. K.; Keiding, S. R.; Thøgersen, J. The Primary Photodynamics of Aqueous Nitrate: Formation of Peroxynitrite. *J. Am. Chem. Soc.* **2003**, *125*, 15571−15576.
(42) Maria, H. J.; McDonald, J. R.; McGlynn, S. P. Electronic Absorption Spectrum of Nitrate Ion and Boron Trihalides. *J. Am. Chem. Soc.* **1973**, *95*, 1050−1056.
(43) Thøgersen, J.; Gadegaard, A.; Nielsen, J.; Jensen, S. K.; Petersen, C.; Keiding, S. R. Primary Formation Dynamics of Peroxynitrite Following Photolysis of Nitrate. *J. Phys. Chem. A* **2009**, *113*, 10488.
(44) Petersen, C.; Thøgersen, J.; Knak Jensen, S.; Keiding, S. R.; Sassi, P. Solvent Response to Solute Photo-dissociation. *Phys. Chem. Chem. Phys.* **2008**, *10*, 990−995.
(45) Tongraar, A.; Tangkawanwanit, P.; Rode, B. M. A Combined QM/MM Molecular Dynamics Simulations Study of Nitrate Anion (NO_3^-) in Aqueous Solution. *J. Phys. Chem. A* **2006**, *110*, 12918.
(46) Paesani, F.; Voth, G. A. The Properties of Water: Insights from Quantum Simulations. *J. Chem. Phys. B* **2009**, *113*, 5702.
(47) Kurochkin, D. V.; Naraharisetty, S. R. G.; Rubtsov, I. V. Multidimensional Ultrafast Spectroscopy Special Feature: A Relaxation-Assisted 2D IR Spectroscopy Method. *Proc. Natl. Acad. Sci. U.S.A.* **2007**, *104*, 14209−14214.
(48) Wynne, K.; Hochstrasser, R. M. Coherence Effects in the Anisotropy of Optical Experiments. *Chem. Phys.* **1993**, *171*, 179−188.
(49) Farrow, D. A.; Smith, E. R.; Qian, W.; Jonas, D. M. The Polarization Anisotropy of Vibrational Quantum Beats in Resonant Pump−Probe Experiments: Diagrammatic Calculations for Square Symmetric Molecules. *J. Chem. Phys.* **2008**, *129*, 174509.
(50) Galli, C.; Wynne, K.; LeCours, S. M.; Therien, M. J.; Hochstrasser, R. M. Direct Measurement of Electronic Dephasing Using Anisotropy. *Chem. Phys. Lett.* **1993**, *206*, 493−499.
(51) Jansen, T. l. C.; Auer, B. M.; Mino, Y.; Skinner, J. L. Two-Dimensional Infrared Spectroscopy and Ultrafast Anisotropy Decay of Water. *J. Chem. Phys.* **2010**, *132*, 224503.
(52) Van der Post, S. T.; Scheidelaar, S.; Bakker, H. J. Femtosecond Study of the Effects of Ions on the Reorientational Dynamics of Water. *J. Mol. Liq.* **2012**, *176*, 22−28.